Optical properties of photonic crystal heterostructure cavity lasers

Antonios V. Giannopoulos[1], Yu-Jia Li[1,2], Christopher M. Long[1,3], Jian-Ming Jin[1], and Kent D. Choquette[1]

[1]*Department of Electrical and Computer Engineering, University of Illinois, Urbana, Illinois 61801*

[2]*Currently with Cadence Design Systems, San Jose, CA 95134*

[3]*Currently with School of Electrical and Computer Engineering, Purdue University, West Lafayette, IN 47907-1285*

giannopo@illinois.edu

Abstract: We design, fabricate, and test photonic crystal heterostructure cavity lasers in the InP material system. A heterostructure cavity is formed by interfacing two different photonic crystals such that a dispersion maximum of the inner lattice lies within the band gap of the surrounding lattice. Feedback to slow light modes of the central region results in a lower threshold and single mode operation. The use of a kagome lattice as the inner defect area increases the semiconductor volume as well as the modal overlap with the gain material. We use a simulation technique to verify experimentally observed single mode operation as well as to quantify the effects of the heterostructure cavity formation.

OCIS codes: (140.5960) Semiconductor lasers; (230.5298) Photonic crystals.

References and links

1. O. Painter, R. K. Lee, A. Scherer, A. Yariv, J. D. O'Brien, P. D. Dapkus, I. Kim, "Two-Dimensional Photonic Band-Gap Defect Mode Laser," Science **284,** 1819–1821 (1999).
2. H. G. Park, J. K. Hwang, J. Huh, H. Y. Ryu, S. H. Kim, J. S. Kim, and Y. H. Lee, "Characteristics of Modified Single-Defect Two-Dimensional Photonic Crystal Lasers," IEEE J. Quantum Electron. **38,** 1353–1365 (2002).
3. Y. Akahane, T. Asanao, B. S. Song, and S. Noda, "High-Q photonic nanocavity in a two-dimensional photonic crystal," Nature (London) **425,** 944–947 (2003).
4. Y. Akahane, T. Asano1, B. S. Song, and S. Noda, "Fine-tuned high-Q photonic-crystal nanocavity," Opt. Express **13,** 1202–1214 (2005), http://www.opticsinfobase.org/oe/abstract.cfm?URI=oe-13-4-1202.
5. K. Nozaki, T. Ide, J. Hashimoto, W. H. Zheng, and T. Baba, "Photonic crystal point-shift nanolaser with ultimate small modal volume," Electron. Lett. **41,** 843–845 (2005).
6. H. Y. Ryu, S. H. Kwon, Y. J. Lee, Y. H. Lee, and J. S. Kim, "Very-low-threshold photonic band-edge lasers from free-standing triangular photonic crystal slabs" Appl. Phys. Lett. **80,** 3476–3478 (2002).
7. C. Monat, C. Seassal, X. Letartre. P Regreny, P. Rojo-Romeo, P. Viktorovitch, M. Le Vassor d'Yerville, D. Cassagne, J. P. Albert. E. Jalaguier, S. Pocas, and B. Aspar, "InP based two-dimensional photonic crystal on silicon: In-plane Bloch mode laser," Appl. Phys. Lett. **81,** 5102–5103 (2002).
8. H. Y. Ryu, M. Notomi, Y. H. Lee, "Finite-difference time-domain investigation of band-edge resonant modes in finite-size two-dimensional photonic crystal slab," Phys. Rev. B **68,** 045209–1–9 (2003).
9. S. H. Kwon, S. H. Kim, S. K. Kim, Y. H. Lee, and S. B. Kim, "Small, low-loss heterogeneous photonic band-edge laser," Opt. Express **12,** 5356–5361 (2004), http://www.opticsinfobase.org/oe/abstract.cfm?URI=oe-12-22-5356.

#106900 - $15.00 USD Received 2 Feb 2009; revised 15 Mar 2009; accepted 16 Mar 2009; published 20 Mar 2009

10. X. Letartre, C. Monat, C. Seassal, and P. Viktorovitch, "Analytical modeling and an experimental investigation of two-dimensional photonic crystal microlasers: defect state (microcavity) versus band-edge state (distributed feedback) structures," J. Opt. Soc. Am. B **22,** 2581–2595 (2005).
11. F. Bordas, M. J. Steel, C. Seassal, and A. Rahamani, "Confinement of band-edge modes in a photonic crystal slab," Opt. Express **15,** 10890–10902 (2007), http://www.opticsinfobase.org/oe/abstract.cfm?URI=oe-15-17-10890.
12. H. T. Hattori, I. McKerracher, H. H. Tan, C. Jagadish, and R. M. De La Rue, "In-Plane Coupling of Light From InP-Based Photonic Crystal Band-Edge Lasers Into Single-Mode Waveguides," IEEE J. Quantum Electron. **43,** 279–286 (2007).
13. A. V. Giannopoulos, C. Long, and K. D. Choquette, "Photonic Crystal Heterostructure Cavity Lasers using Kagome Lattices," Electron. Lett. **44,** 803–804 (2008).
14. Y. J. Li and J. M. Jin, "A vector dual-primal finite element tearing and interconnecting method for solving 3-D large-scale electromagnetic problems," IEEE Trans. Antennas Propag. **54,** 3000–3009 (2006).
15. Y. J. Li and J. M. Jin, "Fast full-wave analysis of large-scale three-dimensional photonic crystal devices," J. Opt. Soc. Am. B **24,** 2406–2415 (2007).

1. Introduction

The progression of fabrication technologies has allowed for the realization of compact and efficient semiconductor lasers. Because of this, micro-cavity semiconductor lasers have been used in a wide variety of applications in communications and sensing, as well as for experiments in cavity quantum electrodynamics. Recently two-dimensional photonic crystals have been pursued as viable candidates for creating micro- and nano-scale lasers [1]. These types of devices utilize a periodic refractive index variation which enables ultra-small modal volumes and low lasing thresholds with high fidelity in their lasing spectrum [2]-[5]. They are suitable for a wide range of integrated applications since their optical characteristics are lithographically tunable.

Two basic characteristics of photonic crystals can be employed to make lasers: photonic band gaps and slow light. Photonic crystal defect cavity lasers rely on the defects of a photonic crystal to act as optical cavities. In this case, the laser relies on the high reflectivity of the photonic crystal at frequencies inside the photonic band gap. Slow light effects at the dispersion symmetry points, or band edges, in photonic crystals can also be used to create lasers [6]-[8]. In band edge lasers the slow group velocity at the dispersion symmetry points acts to increase the interaction time between the optical field and the gain material, effectively enhancing the available optical gain. The modal areas in the plane of a 2-dimensional photonic crystal slab of the photonic crystal defect cavity lasers can range from less than 1 to a few μm^2 and still maintain high spectral fidelity [1]-[5]. In contrast, the resonator area for efficient band edge lasers is generally larger than 100 μm^2 (approximately 300 μm^2 in [6]). While small area defect lasers support only a few modes within the gain bandwidth of the material system, larger area defects can support many modes. Band edge lasers operate with a few modes or a single mode lasing, but are somewhat impractical for micro- and nano-photonics due to the large area required to operate efficiently. Thus there exists an area gap for efficient and high spectral fidelity photonic crystal lasers.

Recent work has indicated that the combination of these two phenomena, photonic band gaps and slow light, can yield promising results [9]-[13]. In particular, the use of the same lattice with regions of two different hole diameters was used to localize a band edge mode within a heterogenous defect, and resulted in low lasing thresholds [9]. The work presented herein focuses on the incorporation of a kagome photonic crystal as the defect area within a hexagonal photonic crystal to form a photonic crystal heterostructure cavity. A scanning electron micrograph of a photonic crystal heterostructure cavity is shown in Fig. 1. The use of a kagome inner lattice allows for an increase in the semiconductor material of the cavity region while maintaining spectral fidelity. The design of the laser is such that a band edge confined mode of the kagome inner lattice is also in the photonic band gap of the surrounding hexagonal lattice. This results

#106900 - $15.00 USD Received 2 Feb 2009; revised 15 Mar 2009; accepted 16 Mar 2009; published 20 Mar 2009

in optical feed back to a slow light mode of the inner region.

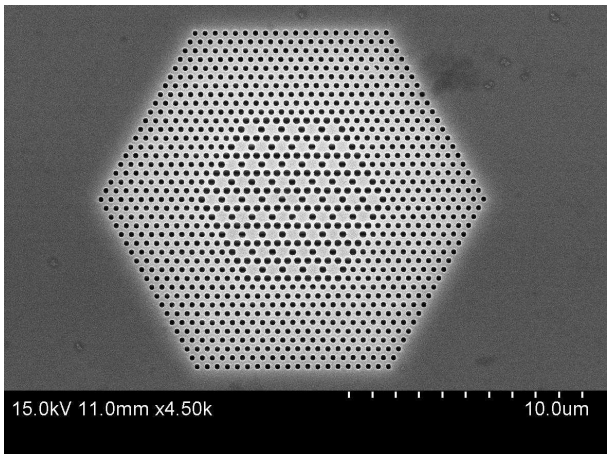

Fig. 1. Scanning electron micrograph of a photonic crystal heterostructure cavity laser.

In this paper, the design, fabrication, and testing of photonic crystal heterostructure cavity lasers using kagome lattices will be discussed. Single mode lasing is observed and explained using simulation techniques. The modal properties of photonic crystal heterostructure cavities are characterized in terms of the cavity size dependence. The effects of the formation of the heterostructure on the optical mode will also be quantified experimentally and numerically.

2. Design by band diagram analysis

One of the main advantages of using a kagome lattice as the inner defect of a photonic crystal heterostructure laser is to increase the overall semiconductor area. Figure 2 shows the percent semiconductor material for kagome (solid) and hexagonal(dashed) 2D lattices as a function of hole radius, r, to nearest neighbor hole spacing, a. The percentage of more semiconductor material in a kagome lattice is also shown (dotted). As the ratio r/a increases, the difference in semiconductor material between the two lattices increases. In the design range of the photonic crystal heterostructure laser this results in the kagome having about 25% more semiconductor material. This is advantageous in that more material provides better mechanical and thermal stability. The main advantage to using the kagome lattice is that for the modes of interest, the kagome lattice has a higher overlap between the semiconductor and the optical field. This leads to a more efficient use of the available material gain. As an example, when $r/a = 0.37$, the overlap of the K-point mode closest to the bottom of the band gap is 78% and 69% for the kagome and hexagonal lattices, respectively. A larger overlap of the mode with the gain material allows for the use of a lower quality factor cavity. This allows more light to escape the cavity without a degradation in device performance. It also allows for the use of material that has a smaller material gain.

The photonic crystal heterostructure cavity using a kagome lattice as the inner defect region and an outer hexagonal lattice can be designed by considering the band diagrams of the two photonic crystals. Figures 3(a) and 3(b) show the band diagrams for a hexagonal lattice and kagome lattice, respectively. In order to avoid lattice mismatch between the kagome and hexagonal regions, a is equal for both lattices. The r/a ratio of each lattice is used to tune the dispersion. The r/a ratios of the kagome and hexagonal lattices are 0.37 and 0.32, respectively, in Fig. 3. The bandgap of the hexagonal lattice which lies between $a/\lambda = 0.259$ to 0.348

#106900 - $15.00 USD Received 2 Feb 2009; revised 15 Mar 2009; accepted 16 Mar 2009; published 20 Mar 2009

is tuned to overlap a dispersion maximum at the K-point of the kagome lattice which lies at $a/\lambda = 0.274$. The high reflectivity of the hexagonal lattice due to the bandgap effect thus provides feedback to the slow light modes at the K-point of the kagome lattice. This results in a decrease of in-plane losses when compared to the case when the hexagonal cladding is absent. Out-of-plane losses are minimized by operation below the light cone of both lattices, shown by the shaded area of Fig. 3. Although analysis of the band diagrams predicts a cavity resonances close to $a/\lambda = 0.274$, a more rigorous simulation is performed as described in Section 4.2.

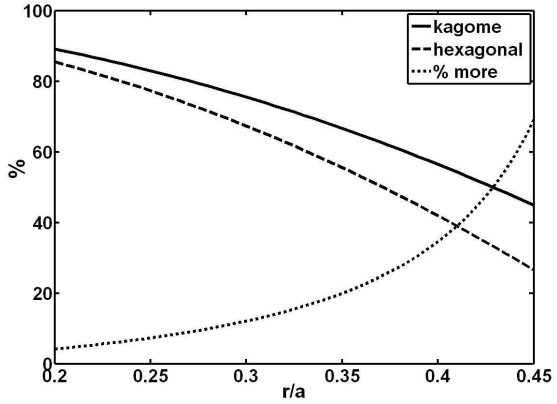

Fig. 2. The percent semiconductor material for a kagome (solid) and hexagonal (dashed) lattices. The percent more semiconductor material is also shown (dotted).

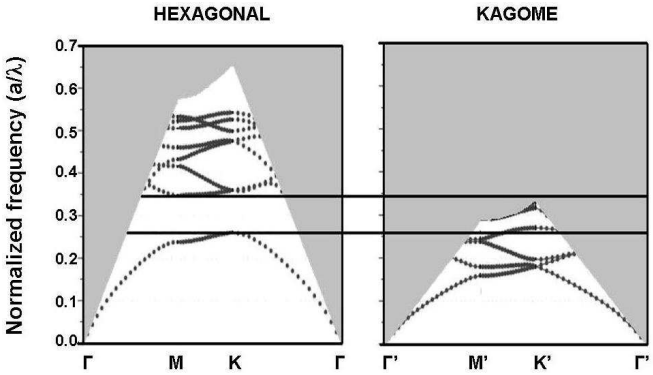

Fig. 3. Photonic band diagrams of a hexagonal(left) and kagome(right) 2D membrane photonic crystal. The grey regions correspond to modes not confined with the membrane. The band gap of the hexagonal lattice (horizontal lines) overlaps the dispersion maximum at the K-point of the kagome lattice.

3. Fabrication

The lasers are fabricated in the InGaAsP/InP material system. Six 5.5 nm thick quantum wells with a photoluminescence peak around 1550 nm are separated by 15 nm thick barriers. A separate confinement heterostructure is formed by surrounding the quantum wells on either side

#106900 - $15.00 USD Received 2 Feb 2009; revised 15 Mar 2009; accepted 16 Mar 2009; published 20 Mar 2009

with wider band gap materials that sum to 84.5 nm thick. A 100 nm sacrificial InP layer is grown on top of the quaternary membrane which is grown on an InP substrate. This layer helps minimize damage to the membrane due to the try etch process.

Fabrication begins with the deposition of a 200 nm layer of SiO_2 using plasma enhanced chemical vapor deposition. Poly(methyl-methacrylate) (PMMA) is then spun on the sample and electron beam lithography (e-beam) is used to create the photonic crystal patterns. The PMMA is developed using a mixture of methyl isobutyl ketone and isopropanol and a CHF_3 (Freon 23) etch is used to transfer the pattern into the SiO2 etch mask. Inductively-coupled plasma reactive ion etching using Cl_2, H_2, and Ar is used to transfer the pattern through the InGaAsP film and into the substrate. A 1:1 mixture of HCl:H_3PO_4 at room temperature or a 4:1 mixture of HCl:deionized water at 4°C is used to undercut the photonic crystal in order to create a suspended membrane.

4. Optical properties of a photonic crystal heterostructure cavity

4.1. Experimental measurement of a 9-period kagome heterostructure

Testing of the lasers is done via optical pumping. A 980 nm fiber coupled laser diode with a collimated output is focused onto the sample using a 20x objective. The cavities are optically pumped using 100 ns pulses on a 1% duty cycle at room temperature. The 20x objective also collects the photonic crystal laser light and couples it into a fiber which is the input to an optical spectrum analyzer.

The photonic crystal heterostructure cavity laser considered in this section is that shown in Fig. 1. There are 9 periods of kagome lattice surrounded by 10 periods of hexagonal lattice. The nearest neighbor hole spacing, a, is 418 nm and the hole radii are 0.37a and 0.32a in the kagome and hexagonal regions, respectively. These design parameters result in a kagome cavity that has an area of 36.7 μm^2 (approximately 15.3 λ^2) of which approximately 63% is semiconductor. The collected power at the lasing wavelength vs. instantaneous pump power is plotted in Fig. 4. The input power has not been calibrated to the pump spot size and a pump spot larger than the cavity is used. The device has a soft turn on with a linearly extrapolated threshold of approximately 8.0 mW. Figure 5 shows the lasing spectrum at 13 mW input power. Single mode lasing is observed at a wavelength of 1551.5nm. The inset in Fig. 5 shows the subthreshold emission spectrum at a pump power of 7.0 mW. A lorentzian fit to the emission spectrum at 7 mW pump power gives a linewidth of approximately 0.64nm (spectrometer limited). Assuming above transparency operation this gives an upper limit to the quality factor of about 2400.

4.2. Calculation of resonant modes

Simulation of the photonic crystal heterostructure cavity lasers requires the use of a large simulation domain. In order to reduce the computation time and increase the computational efficiency, the modes are calculated using the dual-primal finite-element tearing and interconnecting method (FETI-DPEM) as discussed in [14], [15]. The FETI-DPEM uses a full-wave technique based on a domain decomposition implementation of the finite element method. It allows for efficient broadband frequency domain solutions of large-scale electromagnetics problems by exploiting geometrical repetition. The FETI-DPEM is particularly well suited for photonic crystal problems because because the computational cost increases sublinearly with overall domain size in cases where geometrical elements are repeated [15].

Figure 6 shows the calculated modal spectrum of a photonic crystal heterostructure cavity with 9 periods of kagome lattice, $a = 418nm$, and $r/a = 0.37$ and 0.32 for the kagome and hexagonal lattices, respectively. The calculation using the FETI-DPEM is performed by placing a randomly in-plane polarized current sheet in the kagome defect area, sweeping the frequency

#106900 - $15.00 USD Received 2 Feb 2009; revised 15 Mar 2009; accepted 16 Mar 2009; published 20 Mar 2009

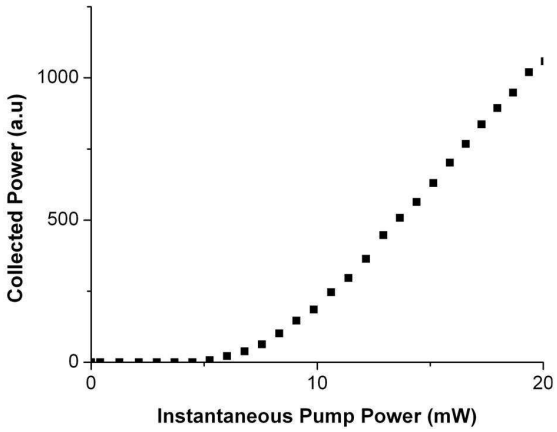

Fig. 4. Collected laser output power as a function of instantaneous pump power at 980 nm.

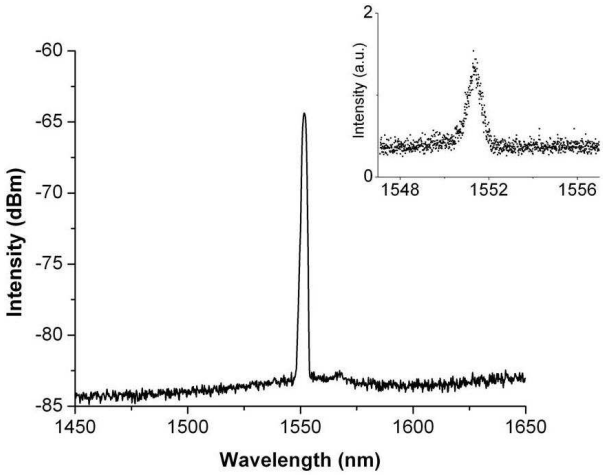

Fig. 5. Lasing spectrum of the photonic crystal heterostructure cavity laser. The inset show the spectrum on a linear scale just below threshold.

of this current, and measuring the stored energy in the cavity. The line widths in Fig. 6 are related to the loss of the particular mode. There are no resonances below approximately 1550 nm due to the overlapping bandgaps of the kagome and hexagonal photonic crystals. The shortest wavelength mode appears at about 1552 nm and there are many modes at longer wavelengths. The intensity profile of the three shortest wavelength modes at 1552 nm, 1560 nm, and 1573 nm are shown in Figs. 7(a)-7(c), respectively. Figures 7(d)-7(f) show the small scale variation near the maxima of the field envelopes.

Even though the calculated spectrum shows many modes above 1550 nm, only one mode at around 1552 nm is experimentally observed in the lasing spectrum. The single mode operation is due to several factors. First, it should be noted that closer proximity to the K-point implies that a given mode should have a smaller group velocity and therefore experience the greatest gain enhancement that the slow group velocity provides. The mode at 1552 nm is closest to

#106900 - $15.00 USD Received 2 Feb 2009; revised 15 Mar 2009; accepted 16 Mar 2009; published 20 Mar 2009

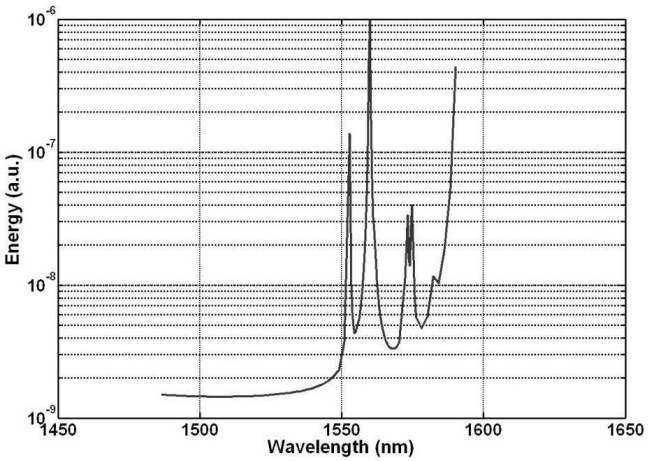

Fig. 6. Calculated stored energy spectrum of a photonic crystal heterostructure cavity laser using the FETI-DPEM.

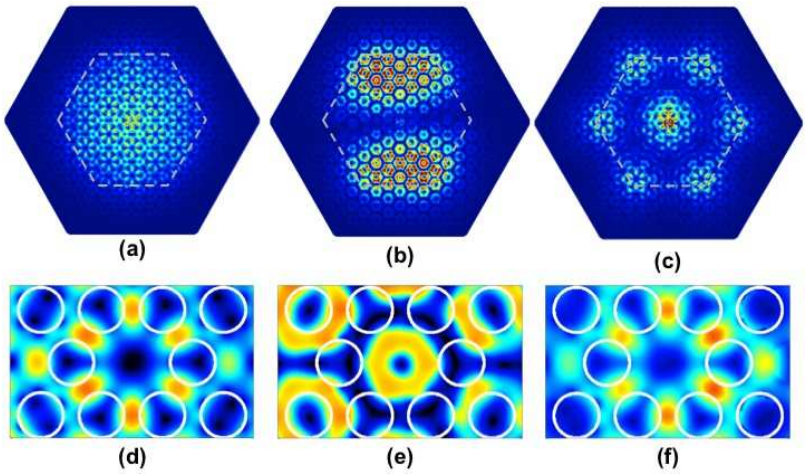

Fig. 7. The calculated modal profiles of the modes at (a) 1552 nm, (b) 1560 nm, and (c) 1573 nm. (d),(e),(f) small scale variation of (a), (b), and (c), respectively

the K-point obtained using the plane wave expansion method. Spatial overlap with the gain and the kagome lattice also needs to be taken into account. The mode at 1552 nm is well confined inside the kagome lattice which is denoted by the dashed lines in Fig. 7. This plays a crucial role since the parts of the field that lie within the hexagonal region experience significant optical loss. When considering the small scale (on the order of a) variation of the field, the mode at 1552 nm looks similar to the hexapole mode often encountered in single defect hexagonal photonic crystal cavities. The field is localized mostly in the semiconductor region away from the holes. The mode at 1560 nm, however, is primarily confined between three adjacent holes and thus greatly overlaps the air holes. The latter mode also will feel the influence of fabrication imperfections more than the shorter wavelength mode. Lastly, the mode at 1552 nm has a well defined intensity maximum at the center of the kagome region and is likely easiest to optically

#106900 - $15.00 USD Received 2 Feb 2009; revised 15 Mar 2009; accepted 16 Mar 2009; published 20 Mar 2009

excite. These criterion in combination lead to single mode lasing as evident in Fig. 5.

4.3. Quality factors of different sized cavities

In this section, simulation of different sized kagome cavities are discussed. The wavelength and quality factors of different sized photonic crystal heterostructure cavities are analyzed using the FETI-DPEM. The relative hole sizes and lattice spacing is the same as the previous section. Resonance and quality factor calculations are performed using the FETI-DPEM. Figure 8 shows the calculated cavity resonances and quality factors for 3, 5, 7, and 9 kagome periods in the inner region of the photonic crystal heterostructure cavity. The wavelength increases slightly as the inner kagome cavity decreases in size. This can be attributed to the uncertainty in dispersion maximum at the K-point of the band diagram. Similar phenomena have been described in [8]. As the size of the kagome region decreases, the distribution of the mode in momentum space increases. As a result, the mode moves away from the dispersion maximum at the K-point to points lower in the band where a larger spread in the momentum vector is supported. Since the mode effectively moves away from the dispersion maximum, it also starts to include momentum-space components with a larger group velocity. This in turn decreases the quality factor as the cavity gets smaller. As the kagome region becomes smaller, the optical mode overlap with the hexagonal cladding region also increases. This causes the mode to experience greater loss as these wavelengths lie with the band gap of the hexagonal cladding. The decrease in quality factor and increase in optical loss for decreasing cavity size is expected to eventually inhibit lasing. Experimentally, photonic crystal heterostructure cavities with inner defect diameters equal to or less than 5 periods did not lase.

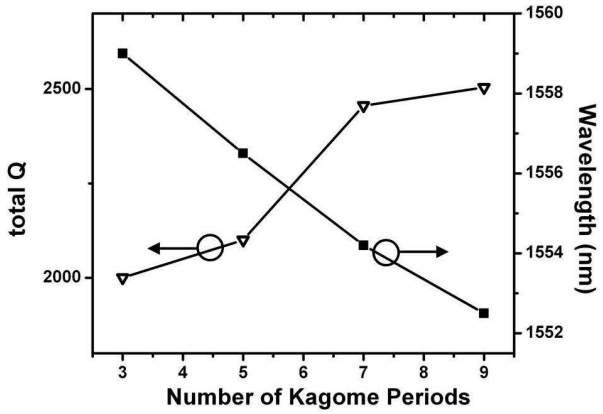

Fig. 8. Resonant wavelength (squares) and quality factor (triangles) of the shortest wavelength mode as a function of the number of kagome inner periods.

4.4. Decomposition of the heterostructure

The photonic crystal heterostructure cavity laser can be experimentally compared to a kagome band edge laser. During heterostructure laser operation, the overlap of the photonic band gap of the exterior hexagonal lattice with the slow group velocity K-point of the kagome lattice dictates the predominant feedback mechanism. It is this union that creates a high quality factor and thus results in laser action. In the absence of the hexagonal cladding, the mode should shift to a longer wavelength do to the decrease in optical confinement. The lack of heterostructure

#106900 - $15.00 USD Received 2 Feb 2009; revised 15 Mar 2009; accepted 16 Mar 2009; published 20 Mar 2009

feedback should also decrease the quality factor at the lasing wavelength and result in a higher threshold pump power.

In order to experimentally confirm the above, a kagome band edge laser identical to the inner region of the photonic crystal heterostructure described in Section 4.1 was fabricated and optically pumped using the same previously mentioned excitation conditions. Figure 9(a) shows the lasing spectra of a photonic crystal heterostructure cavity (solid line) and a kagome band edge laser (dashed). The kagome band edge laser operates at 1592 nm, whereas the photonic crystal heterostructure operates at 1552 nm. Figure 9(b) shows the measured light input vs. light output for the heterostructure (triangles) and kagome band edge (squares) lasers. The kagome band edge laser has a higher threshold than the heterostructure cavity laser. This is attributed to the lack of feedback of the heterostructure resulting in a lower quality factor.

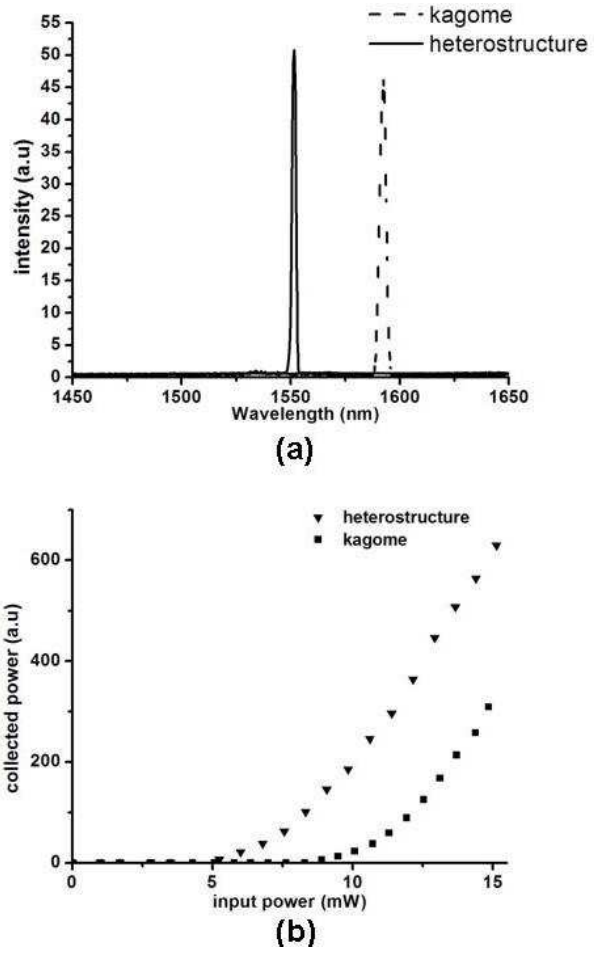

Fig. 9. Comparison between the lasing spectrum(a) and light input vs. light output (b) of a photonic crystal heterostructure and a kagome band edge band edge laser. The kagome band edge band edge laser has a longer lasing wavelength and a higher threshold.

In order to investigate the exact cause of the shift in lasing wavelength, the FETI-DPEM was employed in order to calculate the optical modes of the kagome band edge laser. Figure 10 shows the stored energy as a function of wavelength for the kagome band edge laser. There

#106900 - $15.00 USD Received 2 Feb 2009; revised 15 Mar 2009; accepted 16 Mar 2009; published 20 Mar 2009

are two local maxima at around 1565 nm and 1590 nm that lie within the gain bandwidth of our material. The mode at 1590 nm has a larger quality factor than the mode at 1565 nm. The resonance at 1565 nm has a modal profile similar to that of of the heterostructure lasing mode at 1552 nm (shown in Fig. 7(a)), and the resonance at 1590 nm has a modal profile similar to that of the heterostructure mode at 1560 nm (shown in Fig. 7(b)).

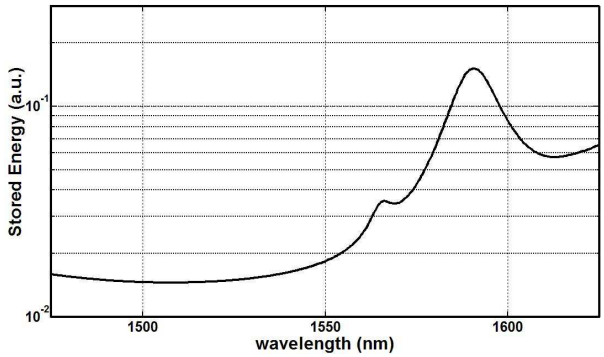

Fig. 10. Stored Energy vs. wavelength for a kagome band edge cavity calculated by the FETI-DPEM.

A comparison between the two lasing modes ($\approx$1552 nm for the heterostructure and $\approx$1590 nm for the kagome band edge laser) is made by considering the distribution of the modes in momentum space. Figures 11(a) and 11(b) show the spatial Fourier transforms of the calculated heterostructure and kagome band edge modes, respectively. To be precise, the sum of the magnitude squared of the Fourier transform of the in-plane electric field components is shown in Fig. 11. For both lasers, the momentum contribution around $k_y = 0$ is from the y-polarized part of the field. The heterostructure mode is seen to contain maxima at the six K-points of the first Brillouin zone. In this case, the mode is strictly localized to near the K-point. This is in contrast to the kagome band edge mode which exhibits a broader momentum space representation. While the kagome band edge mode has momentum localization around the K-points, the momentum space representation actually has nulls at the six K-points. Instead, the mode is spread out and has lobes that contain momentum components in the the K-M and K-Γ directions. This arises presumably from the lack of heterostructure confinement. When a heterostructure is created, there is strong feedback into the central kagome cavity. This in effect makes the kagome region act similarly to a large area kagome photonic crystal. Since the optical mode effectively samples a larger photonic crystal area, the uncertainty in momentum space decreases resulting in a more well defined momentum vector. This also causes a shift toward a shorter wavelength in the kagome lattice since the K-point of interest is a local maximum in the photonic band diagram. The kagome band edge laser on the other hand experiences minimal feedback from the edge of kagome lattice. The result is that the optical modes will contain more momentum space uncertainty and the wavelength will diverge from the K-point. Similar phenomena are described for various sizes of hexagonal lattice band edge lasers in [8].

5. Conclusion

In summary, we have demonstrated the design, fabrication, and operation of a photonic crystal heterostructure cavity laser. The high reflectivity of the photonic band gap of the hexagonal cladding results in high feedback to the central kagome region which operates at the band edge. The FETI-DPEM method was used to calculate the resonant modes and confirm experimental

#106900 - $15.00 USD Received 2 Feb 2009; revised 15 Mar 2009; accepted 16 Mar 2009; published 20 Mar 2009

results. The photonic crystal heterostructure lasers with 9 kagome periods in the central defect exhibit single mode lasing, which was justified with simulation results. Experimental measurements matched well with calculation which indicated a decrease in threshold and wavelength with the formation of the heterostructure. However, both simulation and experiment show that for small enough cavity size, the quality factor decreases and optical loss increases, leading to inoperable lasing. We find that 7 to 9 kagome periods in the central defect leads to efficient single mode lasers. The primary advantages of the heterostructure cavity laser using a kagome lattice is the increase in semiconductor volume and larger modal overlap with the gain material. This allows for a greater mechanical and thermal stability as well as more efficient use of material gain while still providing single mode operation. The larger semiconductor volume would also aid in reducing device resistance were the photonic crystal heterostructure cavity to be implemented as an electrically injected laser.

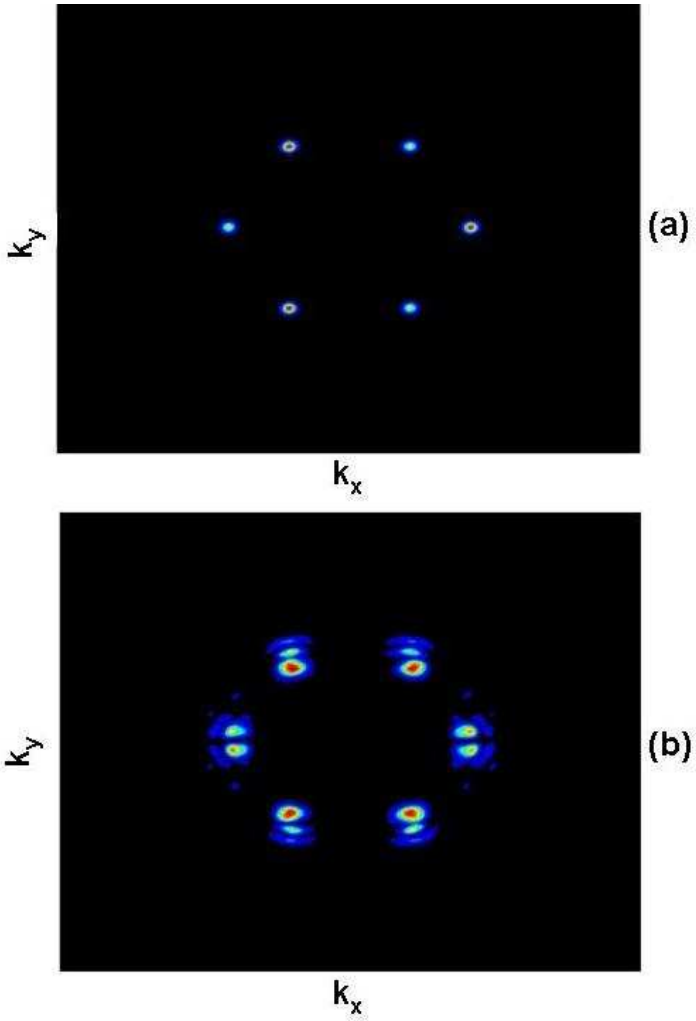

Fig. 11. Fourier space representation of the heterostructure mode at 1552 nm (a) and kagome band edge mode at 1590 nm (b).

#106900 - $15.00 USD Received 2 Feb 2009; revised 15 Mar 2009; accepted 16 Mar 2009; published 20 Mar 2009

Acknowledgment

This work was supported by DARPA under contract number 433143-874 and the National Science Foundation under contract number 07-25515.

#106900 - $15.00 USD Received 2 Feb 2009; revised 15 Mar 2009; accepted 16 Mar 2009; published 20 Mar 2009